Compact Continuous-Variable Entanglement Distillation

Animesh Datta,[1,*] Lijian Zhang,[1,†] Joshua Nunn,[1] Nathan K. Langford,[1] Alvaro Feito,[2] Martin B. Plenio,[3,4] and Ian A. Walmsley[1]

[1]*Clarendon Laboratory, Department of Physics, University of Oxford, OX1 3PU, United Kingdom*
[2]*Vestas Technology Research & Development, Venture Quays, East Cowes, PO32 6EZ, United Kingdom*
[3]*Institut für Theoretische Physik, Albert-Einstein-Allee 11, Universität Ulm, D-89069 Ulm, Germany*
[4]*QOLS, Blackett Laboratory, Imperial College London, Prince Consort Road, SW7 2BW, United Kingdom*

(Received 2 August 2011; published 8 February 2012)

We introduce a new scheme for continuous-variable entanglement distillation that requires only linear temporal and constant physical or spatial resources. Distillation is the process by which high-quality entanglement may be distributed between distant nodes of a network in the unavoidable presence of decoherence. The known versions of this protocol scale exponentially in space and doubly exponentially in time. Our optimal scheme therefore provides exponential improvements over existing protocols. It uses a fixed-resource module—an entanglement distillery—comprising only four quantum memories of at most 50% storage efficiency and allowing a feasible experimental implementation. Tangible quantum advantages are obtainable by using existing off-resonant Raman quantum memories outside their conventional role of storage.

DOI: 10.1103/PhysRevLett.108.060502 PACS numbers: 03.67.Ac, 03.67.Bg, 03.67.Hk, 42.50.Ex

Quantum information science offers a vastly greater information processing capacity than classical information science while using comparable resources [1]. Primary among these resources is the volume of space and duration of time necessary to execute a given task. The scaling of these variables with the problem size distinguishes quantum from classical information processing. This distinction is quickly eroded in the real world, since quantum correlations, which lie at the heart of power of quantum information science, are vulnerable to environmental noise. A critical element of any quantum information system is, therefore, the ability to generate high-quality quantum correlations (i.e., entanglement) between nodes of the system [2] and, equally, to do this in a way so as not to incur unscalable resource consumption. There exists a protocol for this purpose—entanglement distillation [3,4]. Conventional approaches to entanglement distillation are, however, very resource intensive and do not meet a primary criterion for scalable quantum information processing. If it were possible to identify a means to implement entanglement distillation by using a scalable amount of resources, it would be an important step to bridge the gap between in-principle and real-world quantum information science applications.

In this Letter, we introduce the notion of a quantum entanglement distillery, which makes use of quantum memories to enable the same physical space to be used for both the storage and processing of quantum information. For continuous-variable entanglement distillation, it provides improved use of fixed resources to achieve the same levels of improvement in entanglement as earlier schemes. In fact, our distillery has doubly exponential temporal and exponential spatial advantage over existing distillation schemes [4]. It also surpasses crucial limitations of finite-dimensional entanglement pumping schemes [5]. In particular, failed local operations merely reduce the entanglement of the states involved as opposed to a finite-dimensional instance where failed attempts lead to completely unentangled states. Ours is a repeat-until-success scheme using a linear number of initially poorly entangled states to obtain a final state with higher entanglement. The distillery is a fixed module, consisting of only four quantum memories where the final amount of entanglement is governed by the initial states and the number of iterations. Memories [6] allow us to store results from previous iterations while the subsequent ones succeed, providing an exponential advantage in time. The additional exponential advantage in space and time is provided by our entanglement distillation protocol, which we describe later.

The quantum memories not only store quantum information but also process it concurrently in the same physical space. They allow us to repeatedly perform probabilistic operations on the same copy of the quantum state, further saving time and enhancing resilience against decoherence. This is vital, as all local schemes for distilling entanglement must be probabilistic, since entanglement cannot, on average, increase under local operations and classical communications. Furthermore, distillation of continuous-variable entanglement is not possible if all states and operations involved are Gaussian [4,7,8]. A major advantage over finite-dimensional schemes is that failed local operations do not require starting the whole process anew. Our scheme is also event-ready, in that the protocol's success is reported by fixed detector outcomes.

There are two key features the quantum memories must possess to be suitable for our distillery. First, their

time-bandwidth product, which determines the number of iterations that can be executed within their coherence lifetime, must be sufficiently large. Second, they need a transparent failure mode; i.e., they transmit any unstored excitation, allowing them to be used as a beam splitter and enabling *in situ* generation of the initial two-mode squeezed state. Most importantly, at no point do we require a perfect memory. In fact, off-resonant Raman memories [9] satisfy these criteria, providing a clear path to practical implementation of our scheme [10].

We begin by describing our protocol, consisting of two major steps that we call *malting* and *mashing*. We first describe mashing, which provides iterative improvement of a weak entanglement resource, and then the design of our quantum entanglement distillery that implements our scheme. Then we describe malting, the generation of a weak entangled resource, and analyze its success probability. We also show how existing Raman memories suffice in getting close to the limiting state.

Mashing.—The mashing step of entanglement distillation begins with a non-Gaussian resource state $|\psi^0\rangle$. This state is produced in a process called malting, which we describe later. Let us denote it in Schmidt form as

$$|\psi^0\rangle = \sum_n \alpha_n^0 |n\rangle_{A_1} |n\rangle_{B_1}, \tag{1}$$

where $|n\rangle_{A_1}$ ($|n\rangle_{B_1}$) denotes an n-photon Fock state in Alice's (Bob's) mode. This is the resource at the end of malting stage from which we will distill our final state by using an iterative protocol. In the first step of the iteration, Alice and Bob combine two copies of the state $|\psi^0\rangle$ on two 50/50 beam splitters. In the case that each party detects vacuum on one of the emerging modes from each beam splitter, the resultant state in the other two modes is $|\psi^1\rangle$. Next, $|\psi^1\rangle$ is interfered with a fresh copy of $|\psi^0\rangle$ to produce $|\psi^2\rangle$ upon vacuum detection, and so on. At stage i of the protocol, we combine $|\psi^i\rangle$ with $|\psi^0\rangle$ modewise on the beam splitters and detect vacuum, as in Fig. 1(a), to produce the state

$$|\psi^{i+1}\rangle = {}_{A_1B_1}\langle 00|(U_{A_1A_2} \otimes U_{B_1B_2})|\psi^i\rangle_{A_1B_1} \otimes |\psi^0\rangle_{A_2B_2}, \tag{2}$$

where U_{ab} represents a 50/50 beam splitter across modes a and b. If we denote

$$|\psi^i\rangle = \sum_n \alpha_n^i |n\rangle_{A_1} |n\rangle_{B_1}, \quad \text{for } i = 0, 1, 2 \ldots, \tag{3}$$

we obtain, from Eq. (2), an iterative relation of the form

$$\boldsymbol{\alpha}^{i+1} = \mathcal{M}\boldsymbol{\alpha}^i, \tag{4}$$

where $\mathcal{M}$ depends on $|\psi^0\rangle$. The essential mathematical properties of this map and its first few iterations are provided in Ref. [10]. A key innovation of our work is to implement both mashing and malting steps in the same hardware. We call this hardware an entanglement distillery and present a design for it which uses only four quantum memories. Storing the results of the successive probabilistic mashing steps into quantum memories would require them to have 100% storage efficiencies. Our strategy circumvents this demanding requirement by requiring only 50% storage efficiencies.

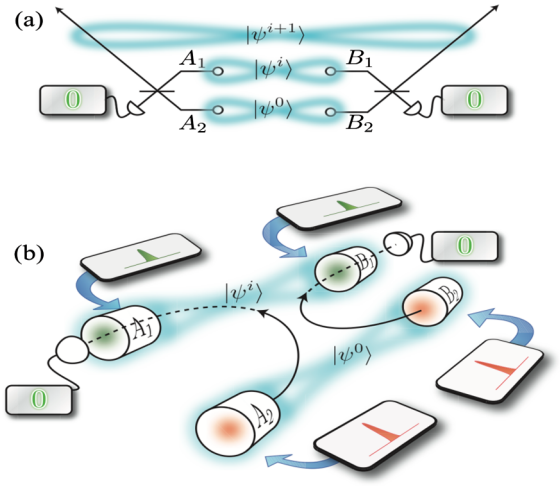

FIG. 1 (color online). Mashing. (a) A linear-optics schematic of the iterative mashing protocol, in which an entangled resource state $|\psi^0\rangle$, distributed between two parties Alice and Bob, is interfered with the shared entangled state $|\psi^i\rangle$ on 50:50 beam splitters. Detection of vacuum by Alice and Bob heralds the success of the protocol, which produces a more entangled state $|\psi^{i+1}\rangle$. (b) Implementation of mashing using four quantum memories. The resource state is generated between memories A_2 and B_2, while the state $|\psi^i\rangle$ is shared between memories A_1 and B_1. The gray panels show the control pulses required to drive the memory interactions: full retrieval (red) and 50:50 beam splitter (green). Mashing is achieved by retrieving the resource state from A_2 and B_2 and sending it through memories A_1 and B_1 while driving a 50:50 beam splitter interaction, as described in the main text. Vacuum detections herald the successful production of $|\psi^{i+1}\rangle$ between A_1 and B_1 (not shown).

An entanglement distillery.—Our distillery consists of four quantum memories to store entangled states during the protocol and act as nonlinear and linear elements for generating and processing them. A quantum memory typically involves three modes: the input, the control, and a localized storage mode. The storage mode b is generally a matter degree of freedom, while the other two are optical. The simplest interaction for transferring a single excitation among three modes is of the form

$$\mathcal{H} \sim a^\dagger b^\dagger c + abc^\dagger. \tag{5}$$

The beam splitter required for the mashing step in Fig. 1(b) can be readily achieved by setting the field a to be classical. Since one of the modes involved is optical, while the other is material, it allows us to exploit the best of both worlds: the optical for transferring information across the distillery and the material for processing it.

Once copies of $|\psi^0\rangle$ are malted between memories A_1 and B_1, and between A_2 and B_2, the matter modes in A_2 and B_2 are converted entirely into optical modes by using strong control pulses. On Alice's side, the photons retrieved from A_2 are directed into A_1 and interfered with the matter mode via a 50/50 beam splitter interaction, as in Fig. 1(b). Correspondingly on Bob's side, the photons retrieved from B_2 are interfered with the matter mode in B_1. In the case that no photons are detected emerging from the ensembles, the state shared by Alice and Bob is projected into $|\psi^1\rangle$. The second iteration proceeds by malting another copy of $|\psi^0\rangle$ between A_2 and B_2 and interfering this with the matter modes in A_1 and B_1 as described above, which produces $|\psi^2\rangle$ provided both Alice and Bob detect vacuum again. The protocol proceeds iteratively. This stage requires a beam splitter interaction with $T = 0$, that is, perfect retrieval [10].

Malting.—A classical mode c in Eq. (5) leads to a two-mode squeezing Hamiltonian between an optical and material mode, the first step of the malting process. It generates a pair of two-mode squeezed states of the form $|\Phi\rangle = \sqrt{1-\lambda^2}\sum_n \lambda^n |n\rangle|n\rangle$, where λ is the squeezing parameter, and the matter mode of each memory is now entangled with its corresponding optical mode. The emitted photons are then directed over the channel connecting Alice and Bob, so that Alice receives Bob's photons, and Bob receives Alice's, as in Fig. 2(a). Each party now uses a control pulse [green pulse in Fig. 2(a)] to drive the same 50/50 beam splitter interaction as used in the mashing step, so that Alice's photons are interfered with Bob's matter modes and vice versa. A photon-counting detector placed behind each memory measures the optical mode emerging from the beam splitter interaction. When no photons are detected, the joint state of the two memories is again a two-mode squeezed state, now between the matter modes of Alice's and Bob's memories [Fig. 2(a)]:

$$|\Phi_{AB}\rangle = \sqrt{1-\lambda^2}\sum_n \lambda^n |n\rangle_A |n\rangle_B. \tag{6}$$

In order to prepare a suitable non-Gaussian resource state $|\psi^0\rangle$, some non-Gaussian operation is now required. That is the aim of the second part of the malting process. To that end, we concentrate on photon subtraction, which has been studied in the context of entanglement distillation previously [4,11].

Photons are subtracted from optical modes by using low-reflectivity beam splitters and photon counters. This is a probabilistic process. In the same way, phonons can be subtracted from the matter modes by sending in weak control pulses and detecting the emission of a photon at the output [Fig. 2(b)]. The advantage of using the matter modes is that the subtraction process can be tried repeatedly on the same copy of the initial state. By contrast, an optical implementation requires fresh preparation of the initial state if the subtraction fails. If, after several weak control pulses [purple pulses in Fig. 2(b)], a photon has been detected by both Alice and Bob, a successful subtraction on matter modes in both the memories has been heralded and our non-Gaussian resource state $|\psi^0\rangle$ is now ready.

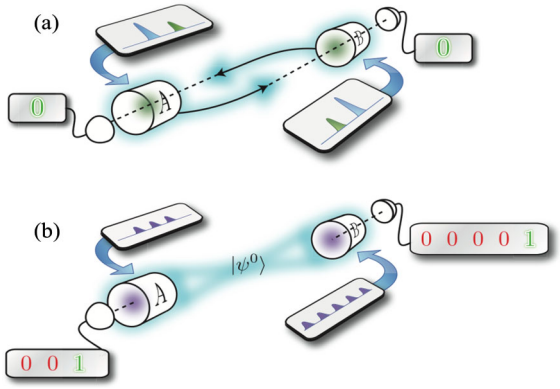

FIG. 2 (color online). Malting. The gray panels show the pulses required to drive the memory interactions: squeezing (blue), 50:50 beam splitter (green), and weak beam splitter (purple). (a) A squeezing interaction in both memories A and B emits photons entangled with spin-wave excitations. The propagating photons from A are directed into B and vice versa, while a 50:50 beam splitter interaction is driven, causing the photons and spin-wave excitations to interfere. Vacuum detections herald the generation of a two-mode squeezed state shared by A and B. (b) De-Gaussification is achieved by photon subtraction at A and B. Because the states are stored in the memories, a repeat-until-success strategy can be employed. Weak control pulses drive a series of beam splitter interactions with small effective reflectivities. When a retrieved photon is detected at both A and B, the malting process is over, and the non-Gaussian entangled resources state $|\psi^0\rangle$ has been successfully generated. The figure shows three and five attempts by A and B, respectively, to successfully implement subtraction. This is a fundamental advantage of a memory-based continuous-variable distillery, without any counterpart in free-space, finite-dimensional distillation schemes.

Each failed detection, however, alters the state. Since the initial state in the memory is a two-mode squeezed state, the quantum state after f vacuum detections (over both arms) is still a two-mode squeezed state of the form of Eq. (6) but with a squeezing parameter of $x = \lambda T^f$, where T is the effective transmissivity of the beam splitter interaction. Rather conveniently, T can be made arbitrarily close to 1 simply by reducing the energy of the subtracting control pulses. If we succeed in detecting photons at the photon counters in Fig. 2(b) after f trials, our resource state takes the (unnormalized) form

$$|\psi^0\rangle = \sum_{n=0}^{\infty} (n+1)\mu^n |n\rangle_{A_1} |n\rangle_{B_1}, \tag{7}$$

with $\mu = xT^2 = \lambda T^{f+2}$. For the initial state $|\psi^0\rangle$, the results of the distillation scheme are presented in Fig. 3.

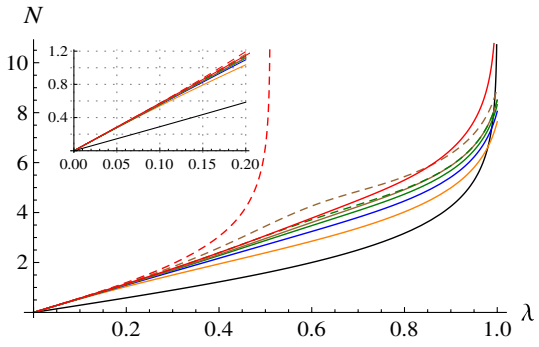

FIG. 3 (color online). Entanglement (logarithmic negativity) after various steps of the distillation protocol. Black curve: Original two-mode squeezed state. Orange curve: Photon subtracted state in Eq. (7). Solid lines: Our scheme. Dashed lines: Exponential scheme of Ref. [4]. Blue curve: 1 iteration; green curve: 2 iterations; brown curve: 3 iterations; red curve: limiting state. Inset: Zoomed into the range $\lambda = [0, 0.2]$. This illustrates the marginal difference in the yield of the two schemes and the appeal of our exponentially improved scheme.

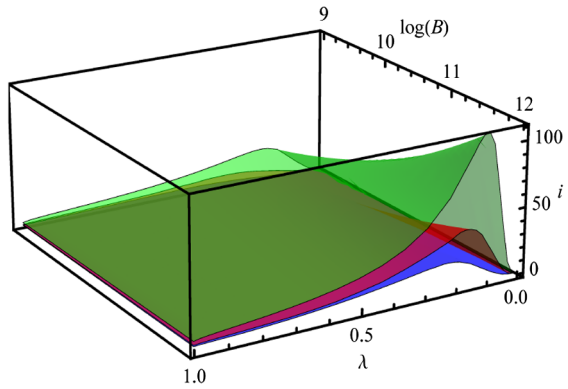

FIG. 4 (color online). Number of iterations possible as a function of the time-bandwidth product B and the initial squeezing λ, for various different values of T used for photon subtraction: $T = 0.8$ (green), $T = 0.9$ (red), and $T = 0.95$ (blue). The smaller the value of T, the larger the maximum number of possible iterations.

Equating this with the entanglement of the initial two-mode squeezed state allows us to find the maximum number of tries f_c within which we must succeed if we are to have a net gain in entanglement. If $T = 1 - \eta$, for small η,

$$f_c \approx \left\lfloor \frac{\log(\lambda/R)}{\eta} \right\rfloor - 2, \tag{8}$$

where R is the real root of the equation $r^3 + (1 - 2\lambda)r^2 + (2 - \lambda)r - \lambda = 0$ [10]. For typical parameters such as $\lambda = 0.2$ and $T = 0.99$, $f_c = 60$. We present the first three iterations of the mashing step using the state in Eq. (7) in Supplemental Material [10].

Implementation in realistic systems.—In practice, the number of iterations in the distillery is limited by the finite storage lifetime t_{mem} of the memories. The utility of a memory is captured by its time-bandwidth product $B = t_{\text{mem}}/\tau$, which is the number of clock cycles, as defined by the duration τ of the control pulses, that fit within the lifetime of the memory. If p_∞^s is the probability of success of mashing two copies of the limiting state, and $\bar{P}_c$ the probability of successful subtraction by trial f_c, the maximum number of iterations i_m satisfies [10]

$$\frac{(i_m + 1)f_c}{\bar{P}_c (p_\infty^s)^{i_m}} \leq B. \tag{9}$$

For $\lambda = 0.15$, $T = 0.75$, and $B = 2500$, $i_m = 12$. Figure 4 shows the number of iterations allowed for a broad range of parameters. From Fig. 3, a small number of iterations, three, for example, suffices to get close to the limiting case. A Raman memory with a time-bandwidth product of $B \sim 2500$ was recently implemented [9], and $B \gtrsim 10^5$ is feasible with modest technical modifications, such as improved magnetic shielding. It has the required properties of high B and a transparent failure mode and can implement Eq. (5) [10]. The pulses in this broadband memory are >300 ps long; single-photon avalanche photodiodes with sufficient response time (150 ps) and efficiency ($> 50\%$) to implement the proposed protocol are well-known [12], and considerably faster response times (18 ps) and higher efficiencies ($> 94\%$) have recently been demonstrated with superconducting nanowire detectors [13]. This Raman memory also has a demonstrated storage efficiency of $\sim 60\%$. With reasonable lifetimes, storage, and retrieval efficiencies, implementation of a distillery is feasible by using this technology. Only $T = 1/2$ is required for interference, so perfect mode matching is not needed, and some attenuation of the control intensity can be accommodated. Perfect storage is never required, and where near-perfect retrieval is desirable, it can be implemented easily with a train of several pulses [10]. This establishes the technical feasibility of each stage of our distillation protocol. Finally, inefficient detectors in our scheme lead to different limiting states in our protocol, but entanglement enhancement is still possible by tuning the subtraction beam splitter [14] without affecting the resource scaling of our protocol.

Discussion.—The task of maintaining coherence across quantum devices is the biggest roadblock to scalable quantum technologies. It would thus be immensely beneficial to store and process quantum information in the same physical space. We show that quantum memories can play this dual role. We have presented a protocol exploiting this duality and identified an existing memory to implement it. We have provided the general criterion required of such a memory. Using just four quantum memories with imperfect storage efficiencies, our quantum distillery can produce high-quality entangled states between distant parties. This can be used to build quantum networks to experimentally study a broad range of quantum phenomena from quantum walks to the simulation of efficient energy transport in light-harvesting complexes [15].

We thank X.-M. Jin for several discussions. This work was funded in part by EPSRC (Grant No. EP/H03031X/1), EU-Mexico Cooperation project FONCICYT (Grant No. 94142), U.S. EOARD (Grant No. 093020), Alexander von Humboldt Foundation, EU Integrated Project Q-ESSENCE, and the EU STREPs HIP and CORNER. I. A. W. acknowledges support from the Royal Society.

*animesh.datta@physics.ox.ac.uk
†lijian.zhang@physics.ox.ac.uk

[1] M. A. Neilsen and I. L. Chuang, *Quantum Computation and Quantum Information* (Cambridge University Press, Cambridge, England, 2000).
[2] L.-M. Duan, M. D. Lukin, J. I. Cirac, and P. Zoller, Nature (London) **414**, 413 (2001); V. Giovannetti, S. Lloyd, and L. Maccone, Nature Photon. **5**, 222 (2011).
[3] C. H. Bennett, H. J. Bernstein, S. Popescu, and B. Schumacher, Phys. Rev. A **53**, 2046 (1996); C. H. Bennett, D. P. DiVincenzo, J. A. Smolin, and W. K. Wootters, *ibid.* **54**, 3824 (1996).
[4] D. E. Browne, J. Eisert, S. Scheel, and M. B. Plenio, Phys. Rev. A **67**, 062320 (2003); J. Eisert, D. E. Browne, S. Scheel, and M. B. Plenio, Ann. Phys. (N.Y.) **311**, 431 (2004).
[5] W. Dür and H. J. Briegel, Rep. Prog. Phys. **70**, 1381 (2007); J. W. Pan, C. Simon, C. Brukner, and A. Zeilinger, Nature (London) **410**, 1067 (2001).
[6] C. Simon *et al.*, Eur. Phys. J. D **58**, 1 (2010).
[7] J. Eisert, S. Scheel, and M. B. Plenio, Phys. Rev. Lett. **89**, 137903 (2002); J. Fiurašek, *ibid.* **89**, 137904 (2002); G. Giedke and J. I. Cirac, Phys. Rev. A **66**, 032316 (2002).
[8] H. Takahashi *et al.*, Nature Photon. **4**, 178 (2010).
[9] K. F. Reim *et al.*, Phys. Rev. Lett. **107**, 053603 (2011); K. F. Reim *et al.*, Nature Photon. **4**, 218 (2010); J. Nunn *et al.*, Phys. Rev. A **75**, 011401 (2007).
[10] See Supplemental Material at http://link.aps.org/supplemental/10.1103/PhysRevLett.108.060502 for (i) convergence of the mashing step of the distillation protocol, (ii) mashing in the presence of dephasing, (iii) the maximum number of subtraction attempts, (iv) the probability of success of the malting step, and (v) Raman memories.
[11] T. Opatrńy, G. Kurizki, and D.-G. Welsch, Phys. Rev. A **61**, 032302 (2000); P. T. Cochrane, T. C. Ralph, and G. J. Milburn, *ibid.* **65**, 062306 (2002); S. Olivares, M. G. A. Paris, and R. Bonifacio, *ibid.* **67**, 032314 (2003); A. Kitagawa, M. Takeoka, M. Sasaki, and A. Chefles, *ibid.* **73**, 042310 (2006).
[12] A. Gulinatti *et al.*, Proc. SPIE Int. Soc. Opt. Eng. **8033**, 803302 (2011).
[13] W. Pernice *et al.*, arXiv:1108.5299.
[14] S. Zhang and P. van Loock, Phys. Rev. A **82**, 062316 (2010).
[15] A. Peruzzo *et al.*, Science **329**, 1500 (2010); F. Caruso *et al.*, J. Chem. Phys. **131**, 105106 (2009); F. Caruso *et al.*, Phys. Rev. A **83**, 013811 (2011).